Assessing the resilience of an electrified transportation network considering failures of charging stations

Hongping Wang[1], Yi-Ping Fang[1], Islam Abdin[1]

[1] Université Paris-Saclay, CentraleSupélec, Laboratoire Génie Industriel, 3 rue Joliot-Curie, 91190 Gif-sur-Yvette, France. E-mail: hongping.wang@centralesupelec.fr; islam.abdin@centralesupelec.fr; yiping.fang@centralesupelec.fr

Enrico Zio[2,3]

[2]Energy Department, Politecnico di Milano, 20156 Milano, Italy.
[3]Mines ParisTech, PSL Research University, CRC, Sophia Antipolis, France. 1 rue Claude Daunesse, 06904 Sophia-Antipolis, France. E-mail: enrico.zio@polimi.it

Many nations are trying to accelerate the deployment of electric vehicles (EVs) on their road networks, in an effort to relieve greenhouse gas emission and shortage of fossil fuels. The number of EVs and charging facilities is expected to increase significantly in the near future, making the existing transportation systems increasingly coupled with the electrical power systems. These growing couplings may bring new stresses and risks to both systems. However, the failure of electric vehicles charging facilities have not been considered. In this context, this paper investigates the resilience of an electrified transportation network (ETN) under potential failures of its supporting charging facilities. Specifically, a two-staged system optimal dynamic traffic assignment model is proposed to describe characteristics of an ETN such as the configuration of charging stations, travel ranges of EVs and the state of charge of EVs. This model is based on the cell transmission model (CTM) and two metrics are presented to quantify the ETN performance under the scenario of charging facility failures. A numerical example is studied to demonstrate the effectiveness of the proposed ETN resilience analysis framework.

Keywords: Electrified transportation network, Resilience analysis, Electric vehicles, Charging stations, Cell transmission model, Dynamic traffic assignment.

1. Introduction

As one of the critical infrastructures, the road transportation network plays a crucial role in our society, for transporting commodities from manufactures to clients and providing travel services for people's daily life. However, the structural facters, unexpected natural disasters (i.e., earthquake and hurricane) and malicious acts render the road transportation network vulnerable to disruptions, which can cause significant loss from both economic and welfare perspectives. Therefore, resilient road networks are required, characterized by the ability to resist and absorb the negative impacts of crises and to recover functionality efficiently.

Since Holling (1973) first conceptualized resilience in the context of ecological systems, this concept has been increasingly introduced to other research domains (Abdin et al., 2019; Fang and Zio, 2019; Wang et al., 2019). The concept of resilience is firstly specified in the context of the transportation system in 2006 by Murray-Tuite (2006). Since then, increasing attention has been devoted to this topic in transportation (Zhang et al., 2019). According to the approaches used in the literature to measure the performance of the system, three main methods can be categorized: optimization-based methods, simulation-based methods and data-driven methods.

For the optimization-based methods, the user equilibrium or system optimal principle are usually employed as convergence rules. For example, Liao et al. (2018) presented an optimization model for resilience under the constraints of budget and traversal time. Zhang et al. (2019) presented a bilevel mathematical optimization model to mitigate the system-wide traffic congestion and increase the system resilience.

For the simulation-based methods, microscopical traffic simulations are performed to simulate the changes in transportation network. Aimsun microsimulation software was

Proceedings of the 30th European Safety and Reliability Conference and the 15th Probabilistic Safety Assessment and Management Conference
Edited by Piero Baraldi, Francesco Di Maio and Enrico Zio
Published by Research Publishing, Singapore.
ISBN: 978-981-14-8593-0; doi:10.3850/978-981-14-8593-0

used in Fountoulakis et al. (2017) to estimate the traffic system comprising both connected and conventional vehicles in highway, under various penetration rates of connected vehicles. Wang et al. (2019) illustrated the safety resilience of expressways by a two-staged modelling approach based on the data obtained from Aimsun.

Different from the other two methods, data-driven methods directly take advantages of the historical data instead of investigating the evolving mechanism of the system. A GPS data-based method was proposed in Donovan and Work (2017) to quantitatively measure the resilience of transportation systems. Qiang and Xu (2019) utilized an empirical approach to assess road network resilience based on the crowdsourced traffic data from Google Maps.

Besides the conventional factors causing disruption that are typically considered in assessing the resilience of the transportation system, new challenges are posed to transportation systems and the world with the advancement of technology and increasing coupling among critical infrastructures. In this scenario, new factors need to be taken into account to explore their influence on the resilience of the transportation system. For instance, Ahmed et al. (2019) evaluated the resilience of the transportation system considering the presence of connected and automated Vehicles.

In this paper, we assume electric vehicles (EVs) are widely used, and also for long trips. The disruption of charging stations (CSs) on the highway is considered. A new traffic optimization model is proposed to track the state of charge (SOC) of EVs and describe the profile of charging stations on the highway, based on the cell transmission model (CTM).

The rest of the article is structured as below. Section 2 introduces the proposed model and presents the two metrics for estimating the impacts of the failures of charging stations on the performance of the transportation system. Section 3 conducts a numerical case study to illustrate the proposed model, followed by Section 4 with concluding remarks and future research directions.

2. Methodology

Since the existing CTM-based traffic models fail to consider the new factors that EVs bring, a linear programming model for the multiple destinations system optimal dynamic traffic assignment problem considering EVs and charging stations (SO-DTA-E&C) is proposed in this paper. The proposed model is able to describe the profile of the charging stations, track the state of charge (SOC) of EVs and assign the system optimal traffic based on the travel range and the charging demand of EVs.

2.1. SO-DTA-E&C

In order to track the state of charge (SOC) of each EV, energy level l is employed to describe the real-time SOC for each EV. Considering the EVs with different battery capacities, the average travel range L_{avg} is used to represent the battery capacity for all EVs. The electricity consumption of EV can be approximated to be a linear function of the distance traveled. Therefore, mileage can be used to quantify the electrical energy level and is used as its unit measurement, for simplicity. The battery capacity is discretized into homogeneous energy levels. Each energy level can supply electric energy for an EV to travel a certain mileage. In this paper, the mileage traveled by an EV using one energy level is used to define the cell length (cl) in the CTM. Based on the above assumptions and settings, the total number of energy levels (L) of each EV can be calculated by the following equation:

$$L = \frac{L_{avg}}{cl} \tag{1}$$

$\mathcal{L}$ is used to represent the set of energy levels $\{1, \cdots, L\}$.

In the original SO-DTA model, only a single destination is considered. This paper introduces an extended version to handle a general network with multiple O-D pairs and considers also the route choice behaviors specifically. $\mathcal{W}$ is used to represent the set of all O-D pairs. $\mathcal{R}$ represents the set of all the paths. $\mathcal{R}^w$ represents the set of the paths that belong to the O-D pair w. A path r is represented by an ordered collection of cells ($\mathcal{P}^r$).

For simplicity, the ordinary, merging and diverging cells defined in the original CTM (Daganzo, 1994, 1995) are called general cells ($\mathcal{C}_G$), since they share the same updating rules in this paper. $N_i(t)$ is defined as the maximum number of vehicles that can be present in general cell i at time t. In order to integrate the electrified component (e.g., charging stations) into the CTM, charging cells ($\mathcal{C}_C$) and queueing cells ($\mathcal{C}_Q$) are originally defined here. Then, a charging station is modelled by a fixed structure where a charging cell is sandwiched between two queueing cells, as shown in Fig. 1.

The charging cells are used to accommodate the vehicles connecting to the chargers. For charging cell i, $NC_i(t)$ is defined as the maximum number of chargers at time t.

Additionally, a new parameter α_i^t is defined to represent the average charging speed at

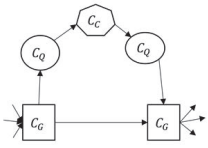

Fig. 1. Cell representation of a charging station.

charging station i at time t. It can be also interpreted as how many energy levels can be supplied at each charger, in charging station i in a time interval τ. Generally, EVs charge faster in a commercial charging station than their energy consumption rate under a common use mode (e.g., no air conditioning). Hence, α_i^t is assumed to be greater than or equal to 1 (energy level per time interval τ). Moreover, for simplicity, α_i^t is rounded to an integer. When a charging station fails, α_i^t is equal to 0, which means no energy can be supplied during failures.

Queueing cells are used to accommodate the vehicles waiting to connect to chargers in the charging stations or waiting to leave the charging stations. Such a structure can prevent the charging cell from being congested and can guarantee it works normally when the downstream general cell is congested. The queueing cell before the charging cell can be regarded as the section from the ramp to the parking lot, and the one after the charging cell can be regarded as the section from the parking lot to the main road, in the service area. We use $NP_i(t)$ to represent the maximum number of parking spaces for queueing cells.

In normal conditions (i.e., without failures), SO-DTA-E&C is formulated in the next subsection.

2.1.1. Formulation of SO-DTA-E&C

The objective function:

$$min \sum_{i\in\{\mathcal{C}\backslash\mathcal{C}_S\}} \sum_{l\in\mathcal{L}} \sum_{r\in\mathcal{R}} \sum_{t\in 0,\cdots,T_h} x_i^{l,r}(t) \tag{2}$$

s.t.

demand satisfaction:

$$\sum_{r\in\mathcal{R}^w} d_i^{l,r}(t) = D_w^l(t), \forall w \in W, t \in 0,\cdots,T_d \tag{3}$$

source cells:

$$x_i^{l,r}(t) = x_i^{l,r}(t-1) + d_i^{l,r}(t-1) - y_{i,j}^{l,r}(t-1), \quad \forall i \in \mathcal{C}_R \cap \mathcal{P}^r, j \in \Gamma_i^+, \forall l \in \mathcal{L}, \forall r \in \mathcal{R},\ t \in 1,\cdots,T_d+1 \tag{4a}$$

$$x_i^{l,r}(t) = x_i^{l,r}(t-1) - \sum_{j\in\Gamma_i^+} y_{i,j}^{l,r}(t-1), \quad \forall i \in \mathcal{C}_R, \forall l \in \mathcal{L},\ \forall r \in \mathcal{R}, t \in T_d+2,\cdots,T_h \tag{4b}$$

general cells:

$$x_i^{l,r}(t) = x_i^{l,r}(t-1) + \sum_{k\in\Gamma_i^-} y_{k,i}^{l+1,r}(t-1) - \sum_{j\in\Gamma_i^+} y_{i,j}^{l}(t-1), \forall i \in \mathcal{C}_G, \forall l \in \{\mathcal{L}\backslash L\}, \forall r \in \mathcal{R}, \forall t \in \mathcal{T} \tag{5a}$$

$$x_i^{L,r}(t) = x_i^{L,r}(t-1) - \sum_{j\in\Gamma_i^+} y_{i,j}^{L,r}(t-1), \quad \forall i \in \mathcal{C}_G, \forall r \in \mathcal{R}, \forall t \in \mathcal{T} \tag{5b}$$

queueing cells:

$$x_i^{l,r}(t) = x_i^{l,r}(t-1) + y_{k,i}^{l,r}(t-1) - y_{i,j}^{l,r}(t-1), \quad \forall k \in \Gamma_i^-,\ \forall j \in \Gamma_i^+,\ \forall i \in \mathcal{C}_Q, \forall l \in \mathcal{L}, \forall r \in \mathcal{R}, \forall t \in \mathcal{T} \tag{6}$$

charging cells:

$$\dot{x}_i^{l,r}(t) = x_i^{l,r}(t-1) + y_{k,i}^{l,r}(t-1) - y_{i,j}^{l,r}(t-1), \forall k \in \Gamma_i^-, \quad \forall j \in \Gamma_i^+,\ \forall i \in \mathcal{C}_C, \forall l \in \mathcal{L}, \forall r \in \mathcal{R}, \forall t \in \mathcal{T} \tag{7}$$

$$x_i^{L,r}(t) = \sum_{s=0}^{\alpha_i^t} \dot{x}_i^{L-\alpha_i^t,r}(t), \quad \forall i \in \mathcal{C}_C, \forall r \in \mathcal{R}, \forall t \in 1,\cdots,T_h, \tag{8a}$$

$$x_i^{l,r}(t) = \dot{x}_i^{l-\alpha_i^t,r}(t), \quad \forall i \in \mathcal{C}_C, \forall l \in \mathcal{L}\backslash\{l < \alpha_i^t, L\}, \forall r \in \mathcal{R}, \forall t \in \mathcal{T}, \tag{8b}$$

$$x_i^{l,r}(t) = 0, \quad \forall i \in \mathcal{C}_C, \forall l \in \{l < \alpha_i^t\}, \forall r \in \mathcal{R}, \forall t \in \mathcal{T}, \tag{8c}$$

links:

$$\sum_{\forall j\in\Gamma_i^+} y_{i,j}^{l,r}(t) - x_i^{l,r}(t) \le 0, \quad \forall (i,j) \in \mathcal{E}, \forall l \in \mathcal{L},\ \forall r \in \mathcal{R},\ \forall t \in \mathcal{T} \tag{9a}$$

$$\sum_{\forall j \in \Gamma_i^+} \sum_l \sum_r y_{i,j}^{l,r}(t) \le Q_i(t), \quad \forall (i,j) \in \mathcal{E}, \forall l \in \mathcal{L},\ \forall r \in \mathcal{R},\ \forall t \in \mathcal{T} \tag{9b}$$

$$\sum_{\forall j \in \Gamma_i^+} \sum_r \sum_l y_{i,j}^{l,r}(t) \le Q_j(t), \quad \forall i,j \in \mathcal{E}, \forall l \in \mathcal{L},\ \forall r \in \mathcal{R}, \forall t \in \mathcal{T} \tag{9c}$$

$$\sum_{\forall i \in \Gamma_j^-} \sum_l \sum_r y_{i,j}^{l,r}(t) + \delta_j(t) \sum_l \sum_r x_j^{l,r}(t) \le \delta_j(t) N_j(t), \quad \forall j \in \mathcal{C} \backslash \mathcal{C}_C \backslash \mathcal{C}_Q, \ i \in \Gamma_j^-,\ \forall l \in \mathcal{L},\ \forall r \in \mathcal{R}, \forall t \in \mathcal{T} \tag{9d}$$

$$\sum_{\forall i \in \Gamma_j^-} \sum_l \sum_r y_{i,j}^{l,r}(t) + \sum_l \sum_r x_j^{l,r}(t) \le N P_j(t), \quad \forall j \in \mathcal{C}_Q,\ i \in \Gamma_j^-,\ \forall l \in \mathcal{L},\ \forall r \in \mathcal{R}, \forall t \in \mathcal{T} \tag{9e}$$

$$\sum_{\forall i \in \Gamma_j^-} \sum_l \sum_r y_{i,j}^{l,r}(t) + \sum_l \sum_r x_j^{l,r}(t) \le N C_j(t), \quad \forall j \in \mathcal{C}_C,\ i \in \Gamma_j^- \forall l \in \mathcal{L},\ \forall r \in \mathcal{R}, \forall t \in \mathcal{T} \tag{9f}$$

initializition

$$x_i^{l,r}(0) = \xi_i,\ \forall i \in \mathcal{C},\quad \forall l \in \mathcal{L}, \forall r \in \mathcal{R} \tag{10}$$

$$y_{i,j}^{l,r}(0) = 0,\ \forall (i,j) \in \mathcal{E},\ \forall l \in \mathcal{L},\ \forall r \in \mathcal{R} \tag{11}$$

$$y_{i,j}^{1,r}(t) = 0,\ \forall (i,j) \in \mathcal{E}, \forall r \in \mathcal{R}, \forall t \in \mathcal{T} \tag{12}$$

$$y_{i,j}^{l,r}(t) = 0,\ \forall (i,j) \in \mathcal{E}_D \cap (i,j) \notin \mathcal{P}^r, \quad \forall r \in \mathcal{R}, \forall t \in \mathcal{T} \tag{13}$$

nonnegative constrains:

$$x_i^{l,r}(t) \ge 0,\quad \forall i \in \mathcal{C},\quad \forall l \in \mathcal{L}, \forall r \in \mathcal{R}, \quad \forall t \in 0, \cdots, T_h \tag{14}$$

$$y_{i,j}^{l,r}(t) \ge 0,\quad \forall (i,j) \in \mathcal{E},\quad \forall l \in \mathcal{L}, \quad \forall r \in \mathcal{R}, \forall t \in 0, \cdots, T_h \tag{15}$$

Considering EVs with different energy levels and destinations, the objective function is to minimize the total travel time over the whole time horizon from a system operator perspective. Eq. (3) guarantees the traffic demand is satisfied over the departure time period: in each time t, the number of departures $d_i^{l,r}(t)$ in cell i with energy level l for O-D pairs w equals to the traffic demand with that energy level and O-D pair. The source cells can store infinite amounts of traffic. They receive traffic directly from the path flow pattern $d_i^{l,r}(t)$. In Eq. (4a), source cells i only belongs to a particular route r of a certain O-D pair w. The cell occupancies for all other source cells which do not belong to the route r are equal to zero. Eq. (4a) considers the period of departure (from time 0 to T_d for variables $d_i^{l,r}(t)$) whereas Eq. (4b) is for the later period without departures. Constraint Eq. (5) expresses the cell mass conservation and gives the specific rules of updating the vehicles occupancies for general cells. Moreover, the path-based and energy-based occupancy for each cell is tracked. Eq. (5a) states that occupancy in general cell i with energy level l at time t equals to its occupancy minus the outflow with the same energy level l, plus the inflow with energy level $l+1$ at the previous time period. This means that when the EVs stay in the same cell or flow out from a cell, their energy levels do not change. Eq. (5b) states that no EVs have higher energy level than the highest energy level, so no EVs' energy is able to keep in the highest level L after flowed into general cell i. Eq. (6) represents the update rule of the queueing cells while ensuring that no energy is consumed by passing through the cell. This is because the consumed energy from a ramp to a parking lot or from a parking lot to the main road is assumed to be negligible compared to the energy consumption of traveling through a cell length. Eq. (7) states the update rule for charging cells occupancy, where $\dot{x}_i^{l,r}(t)$ represents the occupancy of EVs before the SOC of EVs is updated in the charging cell i at time t with energy level l. Eqs. (8a) to (8c) state the update rules for energy levels of EVs in the charging cells. Eq. (8a) states that when the energy levels of EVs are between $[L - \alpha_i^t, L]$, their energy levels are approximately updated as energy level L after a time unit. Eq. (8b) states that when energy levels of EVs are between $[0, L - \alpha_i^t)$, they increase α_i^t energy levels after a time unit. Eq. (8c) ensures that no EVs' energy levels are below α_i^t after being charged for a time unit. Note that the charging cell occupancy is conserved before and after the SOC of the EVs is updated, i.e., $\sum_l \dot{x}_i^{l,r}(t) = \sum_l x_i^{l,r}(t)$. Eqs. (9a) to (9d)

state the specific constraints of determining the flow from cell i to j. Eq. (9e) states that the flow that advances to queueing cells is also constrained by the number of parking spaces remaining $(NP_j(t) - \sum_l \sum_r x_j^{l,r}(t))$ at time t. Similarly, Eq. (9f) states that the flow that can be received by the charging cells is also constrained by the number of available chargers $(NC_j(t) - \sum_l \sum_r x_j^{l,r}(t))$ at time t. Constraint (10) specifies the initial occupancies. Eq. (11) gives the initial flow conditions. Constraint (12) ensures that no EV can exceed their travel ranges. Constraint (13) forces the flow along the links that do not belong to the route r to be zero. Constraints (14) and (15) give the nonnegative conditions.

2.2. A two-stage model for charging station failure

To model the failures of the charging stations, we use α_i^t to represent when and where the failures are, and for how long the corresponding charging stations do not provide service. Other parameters are the same as for the normal conditions. In practice, failures' location and time of occurrence are usually uncertain and unforeseeable; thus, the system's operator is only able to make responses to the failures after they occur. Once a failure occurs, the time required to repair it can be roughly estimated in advance. Therefore, in this paper, we assume that the system operator will immediately receive the failure information (time and location) once it occurs and when the charging service will be recovered. Based on the above assumption, a two-stage model is proposed to represent the optimum system operation under uncertain charging station failure. Let T_f represent the time instance at which a failure occurs. We firstly run SO-DTA-E&C as the first stage (the normal conditions) and it is represented as I. Then, the second stage (the failure) is denoted as II and the optimization model is given as follows.

The objective in case of failures is the same as for the normal conditions, i.e., minimizing the total travel time (Eq. 16):

$$min \sum_{i \in \{\mathcal{C}-\mathcal{C}_S\}} \sum_{l \in \mathcal{L}} \sum_{r \in \mathcal{R}} \sum_{t \in 0,\cdots,T_h} x_{i,II}^{l,r}(t) \quad (16)$$

For the second stage, the following constraints are added based on the results calculated from the first stage problem:

$$x_{i,II}^{l,r}(t) = x_{i,I}^{l,r}(t),\ \forall i \in \mathcal{C},\ \forall l \in \mathcal{L},\ \forall r \in \mathcal{R},\ t \in 0,\cdots,T_f - 1 \quad (17)$$

$$y_{i,j,II}^{1,r}(t) = y_{i,j,I}^{1,r}(t),\ \forall (i,j) \in \mathcal{E},\ \forall l \in \mathcal{L},\ \forall r \in \mathcal{R},\ t \in 0,\cdots,T_f - 1 \quad (18)$$

$$d_{i,II}^{l,r}(t) = d_{i,I}^{l,r}(t),\ \forall i \in \mathcal{C}_{\mathcal{R}},\ \forall l \in \mathcal{L},\ \forall r \in \mathcal{R},\ t \in 0,\cdots,T_f - 1 \quad (19)$$

$$\dot{x}_{i,II}^{l,r}(t) = \dot{x}_{i,I}^{l,r}(t),\ \forall i \in \mathcal{C},\ \forall l \in \mathcal{L},\ \forall r \in \mathcal{R},\ t \in 0,\cdots,T_f - 1 \quad (20)$$

Eqs. (17) to (20) state that the status of the system before the failures occur should be the same as for the normal conditions. After the failures occurred, the route choices and energy needed by the traffic demands that have not departed are replanned according the the current system' status, informed failures' profiles and the constraints of the system operation rules. The response actions include changing the charging stations for some EVs, changing routes for some EVs without charging demands, and that once the failed stations are restored, they are immediately required to provide charging services without delay.

The changes of constraints (3) - (15) are mainly the considered time frame. Specifically, for Eq. (3) and Eq. (4a), t is in $T_f, \cdots, T_d$ and $T_f, \cdots, T_d + 1$, respectively. Eq. (4b) remains the same. Eqs. (5) - (9) and Eqs. (12) - (15), their t is in $T_f, \cdots, T_h$. Eqs. (10) and (11) are not needed.

2.3. Assessment metrics

In order to investigate how charging station failures influence the system performance of the electrified transportation, two performance metrics are proposed. Let κ indicate a charging station failure.

The satisfaction level $\phi^\kappa(t)$ is defined to indicate the extent of the delay caused by the failure κ for all the EVs by time t. The satisfaction level is calculated by the ratio of the actual accumulated arrivals in case of the failure event κ to the expected accumulated arrivals in case of no failure, by time t:

$$\phi^\kappa(t) = \frac{\sum_{i \in \mathcal{C}_S} \sum_{l \in L} \sum_{r \in \mathcal{R}} x_{i,II}^{l,r}(t)}{\sum_{i \in \mathcal{C}_S} \sum_{l \in \mathcal{L}} \sum_{r \in \mathcal{R}} x_{i,I}^{l,r}(t)} \quad (21)$$

If the failure does not make any negative impacts on users' travel time, i.e., everyone reaches their destinations on time by time t,

the satisfaction level $\phi^{\kappa}(t)$ equals to 1. The smaller the value of $\phi^{\kappa}(t)$, the more users are delayed and still on the road by time t.

The charging station utilization $\eta_i(t)$ is defined to illustrate the contribution of the charging station i to EVs charging by time t. The utilization $\eta_{i,I}(t)$ of charging station i by time t under normal conditions is formulated as follows:

$$\eta_{i,I}(t) = \frac{\sum_{s=0}^{t}\sum_{l\in\mathcal{L}}\sum_{r\in\mathcal{R}} x_{i,I}^{l,r}(t)\cdot\alpha_{i,I}^{t}}{\sum_{s=0}^{t}\sum_{i\in\mathcal{C}_C}\sum_{l\in\mathcal{L}}\sum_{r\in\mathcal{R}} x_{i,I}^{l,r}(t)\cdot\alpha_{i,I}^{t}} \tag{22}$$

where $\sum_{s=0}^{t}\sum_{l\in\mathcal{L}}\sum_{r\in\mathcal{R}} x_{i,I}^{l,r}(t)\cdot\alpha_{i,I}^{t}$ means the total number of energy levels (total electric energy) supplied by charging station i by time t. The denominator represents the the total electric energy supplied by all the charging stations by time t

Similarly, the utilization $\eta_{i,II}^{\kappa}(t)$ under failure condition κ can be calculated.

3. An Example

3.1. Data description

This example is originally from Nguyen and Dupuis (1984) network with 13 nodes, 19 links and 4 OD pairs. This road network is modified here by adding 4 charging stations. Its cells' representation, consisting of 48 cells, is shown in Fig. 2. The charging stations are assumed to be only equipped with DC fast chargers and 20 chargers are installed at each station. They provide charging through 480V AC input. They can deliver 60 to 80 miles of range in 20 minutes of charging (DOE, 2019).

We take the time step $\tau = 6$ min and the free-flow speed $v_f = 50$ miles/h. Hence, the cell length is calculated as 6 miles. In 2018, the median of the EV distance ranges on a full charge is estimated to be 125 miles, as reported by the U.S. department of energy (DOE, 2020). This data is used as the average maximum travel range of EVs in this example. Therefore, the total energy levels can be calculated as 25 using Eq. (1). The charging power for each charger is 60 - 80 miles per 20 minutes, i.e., with a charging speed of 3.6 - 4.8 energy levels per time unit. For simplicity, we set $\alpha_{i,I}^{t} = 4$ energy levels per time unit in normal conditions. This study considers a simple failure scenario where charging station 47 is failed at the 10th time step and it is repaired after one hour (20th time step). Hence, this failure event is represented by $\alpha_{47,II}^{t} = 4, t \in \{0,\cdots,9\} \cup \{20,\cdots,60\}$ and $\alpha_{47,II}^{t} = 0, t \in \{10,\cdots,19\}$.

For traffic demands, we assume each O-D pair has same pattern at each time unit; that is, $D_w^l(t) = 0, \forall w \in \mathcal{W}, \forall t \in T_d, l \in \{1,\cdots,4\}$, $D_w^l(t) = 1, \forall w \in \mathcal{W}, \forall t \in T_d, l \in \{5,6\}$, $D_w^l(t) = 2, \forall w \in \mathcal{W}, \forall t \in T_d, l \in \{7,\cdots,10\}$, $D_w^l(t) = 6, \forall w \in \mathcal{W}, \forall t \in T_d, l \in \{11,\cdots,25\}$.

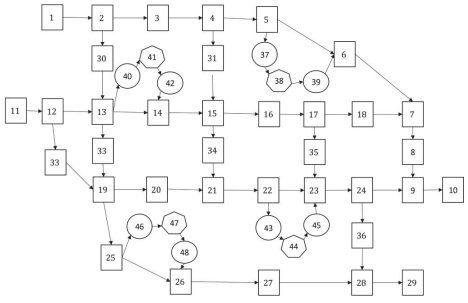

Fig. 2. Cell representation of the studied road network.

Table 1. Parameters used in this example.

Parameters	Values
v_f (m/h)	65
τ (min)	6
cl (mile)	5
ξ_i	0
δ	1
Number of cells	48
Number of chargers	80
Q_i (v/ τ)	200
N_i (v)	1000
NC_i (v)	20
NP_i (v)	100
$\alpha_{i,I}^{t}$	4
L_{avg} (mile)	125
L	25
T_d (min)	20
T_h (min)	600
T_f	10

3.2. Results

The objective value for the first stage is 79109.75, whereas it is 80576.5521 for the second stage, which means the accumulative delayed time for all users is 880.08 hours under the failure event.

Based on the obtained results and Eq. (3), the evolution in time of the satisfaction level

is drawn in Fig. 3. The red vertical line indicates when the failures occurred. Since the satisfaction level indicates the extent of the users delay at destinations, the performance of the system does not decrease immediately when the failure occurs and its response lag behind the development of the failures, as shown in Fig 3, where the station fails at the 10th time step and is restored at the 20th time step, the satisfaction level decreases at about the 15th time step and keeps this trend until around the 24th time step. Then, the satisfaction level gradually oscillates back to the normal conditions.

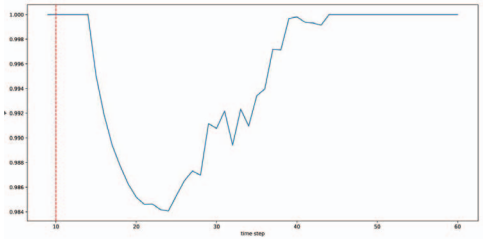

Fig. 3. Evolution of satisfaction level with time.

Fig. 4 shows the evolution of the charging station utilization along with time. The lines with the same color denote the same charging station's utilization. The markers of the circle and cross denote the normal and the failure conditions, respectively. As shown in Fig. 4, charging station 41 always contributes the most charging service for EVs among all the charging stations. After failures occurred, the utilization rate of charging station 47 immediately decreases and the utilization rates of other charging stations increase to varying degrees. Among them, the utilization rate of charging station 41 increases the most. After the failed station is repaired, the utilization rate of charging station 47 gradually increases but is still less than that of the normal conditions. It means some EVs change the routes and chose to charge in other charging stations, because of the failures.

4. Conclusion

This paper proposes a system optimal dynamic traffic assignment model, which is able to describe the profiles of charging stations, travel ranges of EVs and SOC of EVs at each time step. Considering potential failures in the charging stations, a two-stage model is proposed to represent the uncertain nature of failures. In order to assess the resilience of the ETN, two metrics are presented to

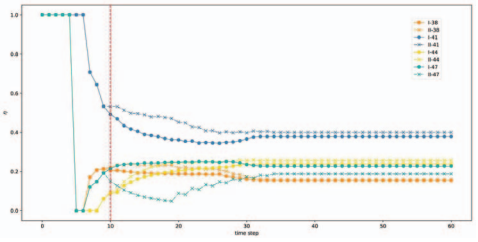

Fig. 4. Evolution of charging station utilization with time.

quantify the impacts of the failures on the ETN. Through an example, it is shown that the critical charging stations can be identified and the evolution of the performance of the ETN over time can be observed.

Other topics for further research could include user equilibrium conditions, optimal allocation of charging stations considering constraints from the electric distribution system and the ETN, and uncertainties in traffic demand.

Acknowledgement

The participation of Hongping Wang to this research is supported by China Scholarship Council (No. 201606990003). The participation of Enrico Zio to this research is supported by the Energy for Motion project of the Department of Energy of Politecnico di Milano, funded by the Italian Ministry of University and Research (MUR) through the Department of Excellence grant 2018-2022.

References

Abdin, I., Y.-P. Fang, and E. Zio (2019). A modeling and optimization framework for power systems design with operational flexibility and resilience against extreme heat waves and drought events. Renewable and Sustainable Energy Reviews 112, 706–719.

Ahmed, S., K. Dey, and R. Fries (2019). Evaluation of transportation system resilience in the presence of connected and automated vehicles. Transportation Research Record 2673(9), 562–574.

Chiou, S.-W. (2020). A resilience-based signal control for a time-dependent road network with hazmat transportation. Reliability Engineering & System Safety 193, 106570.

Daganzo, C. F. (1994). The cell transmission model: A dynamic representation of highway traffic consistent with the hydrodynamic theory. Transportation Research Part B: Methodological 28(4), 269–287.

Daganzo, C. F. (1995). The cell transmission model, part ii: network traffic. Transporta-

tion Research Part B: Methodological 29(2), 79–93.

DOE (2019). office of energy efficiency & renewable energy. https://www.energy.gov/eere/electricvehicles/vehicle-charging. Accessed Feb. 28, 2020.

DOE (2020). Office of energy efficiency & renewable energy. https://www.energy.gov/eere/vehicles/articles/fotw-1064-january-14-2019-median-all-\electric-vehicle-range-grew-73-miles. Accessed Feb. 28, 2020.

Donovan, B. and D. B. Work (2017). Empirically quantifying city-scale transportation system resilience to extreme events. Transportation Research Part C: Emerging Technologies 79, 333–346.

Fang, Y.-P. and E. Zio (2019). An adaptive robust framework for the optimization of the resilience of interdependent infrastructures under natural hazards. European Journal of Operational Research 276(3), 1119–1136.

Faturechi, R. and E. Miller-Hooks (2014). A mathematical framework for quantifying and optimizing protective actions for civil infrastructure systems. Computer-Aided Civil and Infrastructure Engineering 29(8), 572–589.

Feng, K., Q. Li, and B. R. Ellingwood (2020). Post-earthquake modelling of transportation networks using an agent-based model. Structure and Infrastructure Engineering, 1–15.

Fountoulakis, M., N. Bekiaris-Liberis, C. Roncoli, I. Papamichail, and M. Papageorgiou (2017). Highway traffic state estimation with mixed connected and conventional vehicles: Microscopic simulation-based testing. Transportation Research Part C: Emerging Technologies 78, 13–33.

Holling, C. S. (1973). Resilience and stability of ecological systems. Annual review of ecology and systematics 4(1), 1–23.

Liao, T.-Y., T.-Y. Hu, and Y.-N. Ko (2018). A resilience optimization model for transportation networks under disasters. Natural hazards 93(1), 469–489.

Liu, W. and Z. Song (2019). Review of studies on the resilience of urban critical infrastructure networks. Reliability Engineering & System Safety, 106617.

Mojtahedi, M., S. Newton, and J. Von Meding (2017). Predicting the resilience of transport infrastructure to a natural disaster using cox's proportional hazards regression model. Natural Hazards 85(2), 1119–1133.

Murray-Tuite, P. M. (2006). A comparison of transportation network resilience under simulated system optimum and user equilibrium conditions. In Proceedings of the 2006 Winter Simulation Conference, pp. 1398–1405. IEEE.

Nguyen, S. and C. Dupuis (1984). An efficient method for computing traffic equilibria in networks with asymmetric transportation costs. Transportation Science 18(2), 185–202.

Qiang, Y. and J. Xu (2019). Empirical assessment of road network resilience in natural hazards using crowdsourced traffic data. International Journal of Geographical Information Science, 1–17.

Renne, J., B. Wolshon, P. Murray-Tuite, and A. Pande (2019). Emergence of resilience as a framework for state departments of transportation (dots) in the united states. Transportation Research Part D: Transport and Environment.

Tang, D., Y.-P. Fang, E. Zio, and J. E. Ramirez-Marquez (2019). Resilience of smart power grids to false pricing attacks in the social network. IEEE Access 7, 80491–80505.

Vodopivec, N. and E. Miller-Hooks (2019). Transit system resilience: Quantifying the impacts of disruptions on diverse populations. Reliability Engineering & System Safety 191, 106561.

Wang, H., Y.-P. Fang, and E. Zio (2019). Risk assessment of an electrical power system considering the influence of traffic congestion on a hypothetical scenario of electrified transportation system in new york stat. IEEE Transactions on Intelligent Transportation Systems.

Wang, J., Y. Kong, and T. Fu (2019). Expressway crash risk prediction using back propagation neural network: A brief investigation on safety resilience. Accident Analysis & Prevention 124, 180–192.

Zhang, X., S. Mahadevan, and K. Goebel (2019). Network reconfiguration for increasing transportation system resilience under extreme events. Risk analysis 39(9), 2054–2075.

Zhang, X., S. Mahadevan, S. Sankararaman, and K. Goebel (2018). Resilience-based network design under uncertainty. Reliability Engineering & System Safety 169, 364–379.

Zhang, Z., B. Wolshon, and P. Murray-Tuite (2019). A conceptual framework for illustrating and assessing risk, resilience, and investment in evacuation transportation systems. Transportation research part D: transport and environment 77, 525–534.

Zhou, Y., J. Wang, and H. Yang (2019, Dec). Resilience of transportation systems: concepts and comprehensive review. IEEE Transactions on Intelligent Transportation Systems 20(12), 4262–4276.